CHEMISTRY OF MATERIALS

COMMUNICATION

pubs.acs.org/cm

New Anode Framework for Rechargeable Lithium Batteries

Jian-Tao Han,[†,§] Yun-Hui Huang,[‡] and John B. Goodenough[†,*]

[†]Texas Materials Institute, ETC 9.102, University of Texas at Austin, Austin, Texas 78712, United States

[‡]School of Materials Science and Engineering, Huazhong University of Science and Technology, Wuhan 430074, P.R. China.

Supporting Information

KEYWORDS: lithium battery, framework, Li-insertion anode, $TiNb_2O_7$

The output of a battery is a current I at a voltage V for a time Δt that depends on the total electronic charge Q transferred from the anode to the cathode in a full discharge at a constant operating current I. A critical parameter for a portable battery is the energy density QV/W, where W is the weight of the battery and $V = V_{oc} - \eta$ is reduced from its open-circuit value V_{oc} by the polarization $\eta = \eta(I, q)$. For a hand-held device, the volumetric energy density $QV/$volume is also important. In order to minimize η, present-day lithium-ion rechargeable batteries use a liquid-carbonate electrolyte because these nonaqueous liquids dissolve a high concentration of Li salts to give a Li^+-ion conductivity $\sigma_{Li} \approx 10^{-3}$ S/cm. However, these electrolytes are reduced by anodes having a voltage $V \leq 1.0$ V versus Li^+/Li^0 unless the anode is passivated by a Li-permeable solid-electrolyte interface (SEI) layer. The SEI layer formed on a lithium anode prevents uniform plating out of Li during charge, and on repeated charge/discharge cycling, dendrites forming on the anode can grow across the separator to short-circuit a cell and set fire to the flammable electrolyte. Therefore, a lithium anode is only used in a "half-cell" to obtain the performance of a candidate electrode.

Insertion of Li^+ ions into a graphitic carbon is a staging process of C to LiC_6, which gives a flat $V \approx 0.2$ V versus Li^+/Li^0. Therefore, carbon or a carbon-buffered Li alloy is used as the anode where a high battery voltage is required. However, a LiC_6 charged anode forms a passivating SEI layer that, though permeable to Li, consumes Li^+ ions from the cathode unless the SEI layer is preformed on the anode before cell assembly. The solid cathodes of existing rechargeable lithium-ion batteries are all insertion compounds of limited capacity to receive Li^+ ions into their host structure, which means that formation within the cell of the SEI layer on a carbon anode reduces further the limited specific capacity Q/W of a cell. Moreover, the rate of Li transfer across the SEI layer must compete with the rate of Li plating on the surface of the SEI layer where the voltage during charge raises the electron potential above that of Li^+/Li^0. If the Li transfer across the SEI layer is not fast enough to prevent plating out of lithium on the anode during a fast charge, dendrite formation may short-circuit the cell, which limits the safe charging rate of the battery. These problems associated with an SEI layer[1−3] are found wherever the voltage of the anode is $V < 1.0$ V versus Li^+/Li^0.

The spinel $Li_4Ti_5O_{12}$ is reported to be a stable anode operating on the Ti(IV)/Ti(III) redox couple[4] located at 1.5 V versus Li^+/Li^0; it is capable of a fast charge and a long cycle life because no SEI layer is formed. However, it has a low specific capacity (~140 (mA h)/g), and the loss of 1.3 V relative to carbon reduces the energy density of a cell using this anode. Therefore, there is a motivation to identify a solid anode with a higher capacity and having a voltage in the range of $1.1 \leq V \leq 1.5$ V versus Li^+/Li^0. To this end, we have been investigating the Nb(V)/Nb(IV) couple in oxides.[5] In this paper, we report on a new Li-insertion anode TNO having a Wadsley[6] shear structure. The size, the carbon coat of the electrode materials, and the layered spacing are shown in Figure 1c−e, respectively. Our strategy in this work was threefold: (i) the monoclinic ($C2/m$) TNO crystal structure[7] (Figure 1a) possesses disordered Nb and Ti atoms and a 2D interstitial space for Li insertion; moreover, provided ~5 Li/formula unit can be inserted, it would provide a high theoretical capacity of 387.6 (mA h)/g for overlapping Ti(IV)/Ti(III), Nb(V)/Nb(IV), and Nb(IV)/Nb(III) redox couples; (ii) replacing

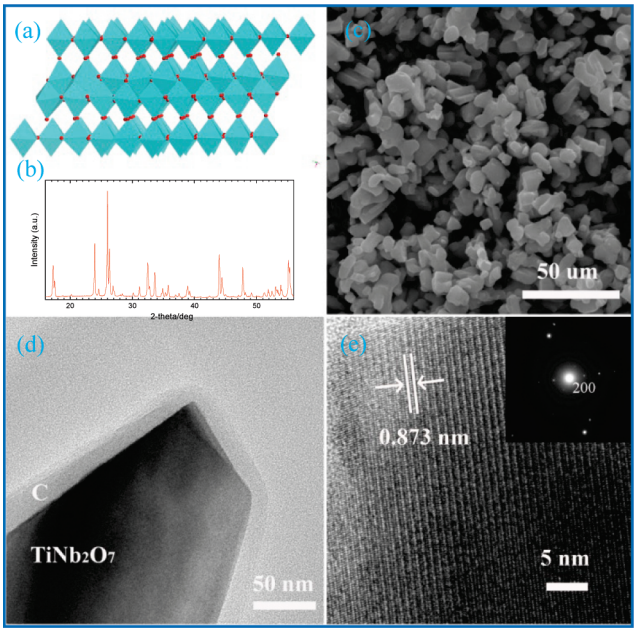

Figure 1. (a) Crystal structure view of TNO, lattice parameters in $C2/m$ space group, $a = 20.351(3)$ Å, $b = 3.801(2)$ Å, $c = 11.882(2)$ Å, $\alpha = \gamma = 90°$, $\beta = 120.19(1)°$ (48109-ICSD). (b) X-ray powder diffraction patterns of TNO. (c) SEM image of bare TNO sample; (d) TEM image of C-TNO sample. (e) HR-TEM image of C-TNO sample; the inset shows the corresponding SAED pattern.

Received: February 11, 2011
Revised: March 24, 2011
Published: March 29, 2011

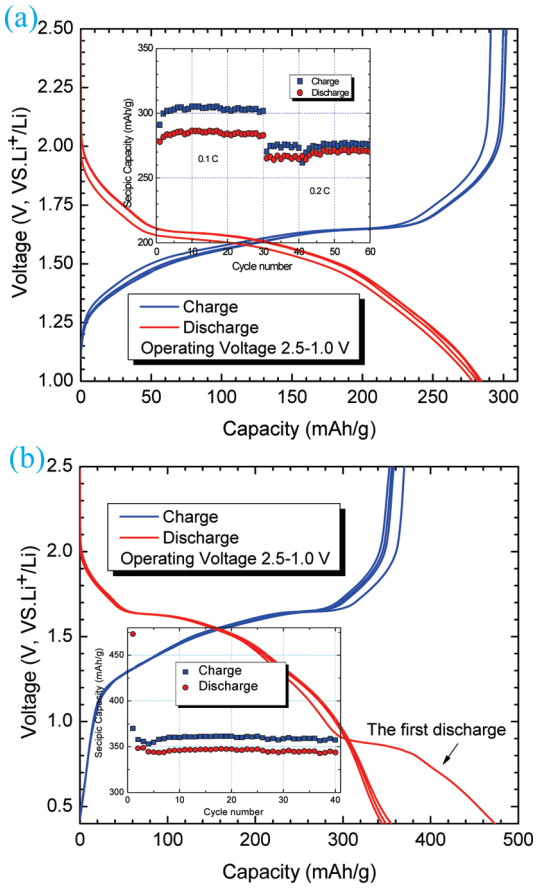

Figure 2. (a) Charge/discharge curves of the C-TNO anode at 0.1 C cycled between 1.0 and 2.5 V, together with its capacity retention over 30 cycles. (b) Charge/discharge curves of the C-TNO anode at 0.1 C cycled between 0.4 and 2.5 V, together with its capacity retention over 40 cycles.

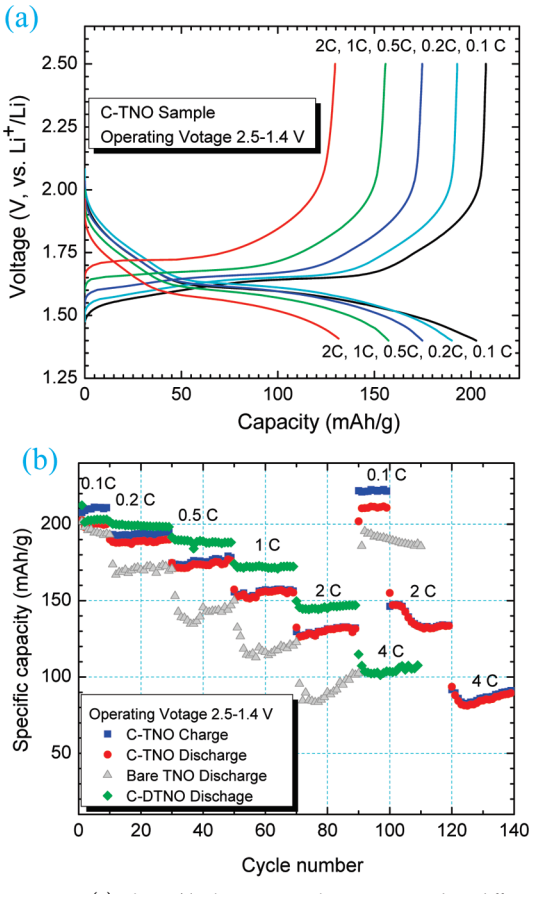

Figure 3. (a) Charge/discharge curves the C-TNO anode at different current densities. (b) Capacity retention of the bare TNO, C-TNO, and C-DTNO anodes at different current densities.

10% Ti(IV) with Nb(IV) can be expected to transform insulating TNO into conducting DTNO; and (iii) carbon coating not only improves the composite electronic conductivity; it also helps to stabilize the Nb(IV) valence state.

TNO was prepared by a sol−gel technique; Nb_2O_5 (Alfa, 99.9%), hydrofluoric acid (40/70 HF/H_2O), $Ti(OC_3H_7)_4$, ammonia, and citric acid monohydrate were used as starting materials. The key step of this process was to obtain a Nb(V) solution. First, Nb_2O_5 was dissolved in hydrofluoric acid to form a transparent solution. In order to remove the F^- ions from the solution, ammonia was added to obtain a white $Nb(OH)_5$ precipitate. After the precipitate was washed and dried, the $Nb(OH)_5$ was dissolved in citric acid to form a Nb(V)−citric solution. We added a water−ethanol solution containing $Ti(OC_3H_7)_4$ to this solution while the pH value of the solution was adjusted by adding ammonia. This final mixture containing Nb(V) and Ti(IV) ions was stirred to form a citric gel at 90 °C; this gel was heated to 140 °C to obtain the precursor. The precursor was annealed at 900−1350 °C to obtain the TNO product. DTNO was prepared by conventional solid state reaction. Stoichiometric quantities of the starting materials, Nb_2O_5 (Alfa, 99.9%), Nb (Alfa, 99.9%), and TiO_2 (Alfa, 99.9%), were thoroughly ground and pressed into pellets. The pellets were wrapped in Ta foil, sealed in a vacuum quartz tube, and annealed at 900−1100 °C for 24 h. C-TNO and C-DTNO were prepared by ball-milling the as-prepared samples into very fine powder and then adding a sucrose solution. Solutions with different concentrations of sucrose were dried at 80 °C before the precursors were annealed at 550 °C for 6 h in a flowing argon atmosphere.

Figure 2a shows the representative charge and discharge voltage profiles of a Li/C-TNO cell cycled between 1.0 and 2.5 V. On the initial discharge, the voltage drops smoothly to 1.0 V with a plateau at 1.6 V versus Li^+/Li^0 and exhibits a capacity of 2.6 Li/formula unit in the voltage range $1.6 > V > 1.0$ V. The cutoff voltage was located at 1.0 V to avoid the formation of an SEI layer. After the first charge, the entire uptake of Li is removed on discharge with a reversible capacity of 285 (mA h)/g, which indicates that, indeed, no SEI layer is formed if the discharge is stopped at $V = 1.0$ V. The inset of Figure 2a shows an excellent Coulombic efficiency of energy storage, over 98%, at a discharge/charge rate of 0.2 C over 30 cycles with no capacity fade.

Figure 2b shows the first discharge to 0.4 V; the irreversible profile below 0.9 V on the first discharge indicates formation of an SEI layer at $V \leq 0.9$ V. Subsequent cycles exhibit a reversible capacity of about 350 (mA h)/g, which shows that the Li-permeable SEI layer protects the surface of the electrodes from further reduction of the electrolyte.

Figure 3a shows the representative charge and discharge voltage profiles of the C-TNO anode at various current densities and cycled between 2.5 and 1.4 V versus Li^+/Li^0. With an increase of current density, the charge potential of the C-TNO anode increased and the discharge potential decreased, rendering a higher overpotential. The cell was first cycled at a low current density of 0.1 C for 10 cycles, where a stable specific capacity of ~200 (mA h)/g (Figure 3b) was

dx.doi.org/10.1021/cm200441h |*Chem. Mater.* 2011, 23, 2027–2029

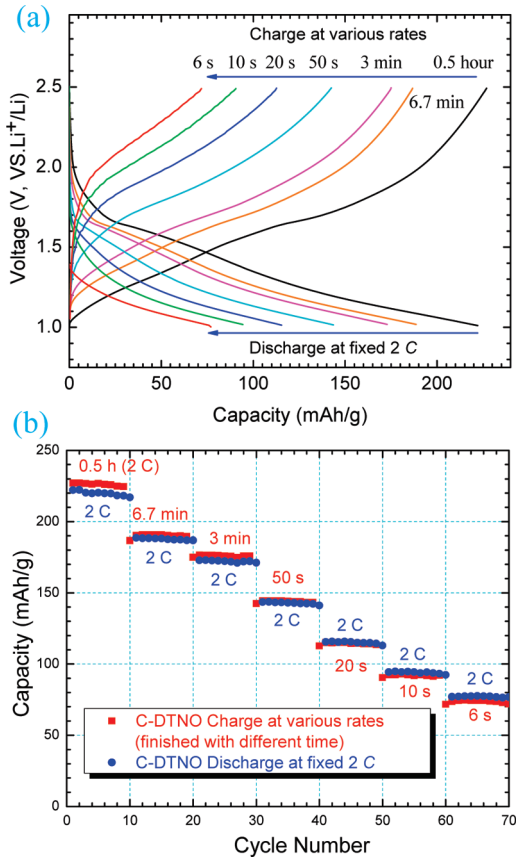

Figure 4. (a) Charge/discharge curves the C-DTNO anode at different current densities. (b) Capacity retention of the C-DTNO anode at high rate: discharge current fixed to give 2 C without any holding of the voltage, charge at very high rate until the charging time reaches 6 s.

obtained. The C-TNO anode showed good rate performance as well. The capacity was as high as ~175 (mA h)/g after we increased the current density by 10 times. Even at a high current density of 2 C, the specific capacity was ~150 (mA h)/g, still higher than the capacity of the $Li_4Ti_5O_{12}$ anode (~140 (mA h)/g). To enhance further the electrochemical properties of the C-TNO anode, we substituted 10% Nb(IV) for Ti(IV) in the TNO composition by solid-state synthesis. The resistance of the DTNO sample was tested by a four-probe measurement to be 0.1 Ω·cm at room temperature (see Supporting Information Figure S2). The cycle performances of the TNO, C-TNO, and C-DTNO anodes are shown in Figure 3b. We observed that the electrochemical performance of the C-DTNO is better than that of bare TNO and C-TNO, which is due to the intrinsic and extrinsic conductivity improvement by atom substitution and carbon-coating.

In order to establish the true rate capability of the active material, carbon black was added in a standard electrode fabrication with 30 wt % carbon black and 5 wt % binder to facilitate electron transport from the active material to the current collector. Figure 4a shows the electrochemical performance of the C-DTNO anode at high charging rate. The discharge rate is fixed at 2 C, and charging rates were increased gradually. The results (see Figure 4a) show that extremely high charging rates can be achieved for the active material: more than 100 (mA h)/g capacities can be achieved at a 20-s total charge; 70 (mA h)/g can still be obtained at a 6-s full charge. Such charging rates are comparable to that of the results reported for the $Li_4Ti_5O_{12}$ anode.[8]

In conclusion, we report a new high-rate Li-insertion anode material for Li-ion batteries charging potential located at 1.3−1.6 V versus Li^+/Li^0 that is fully reversible where no SEI layer is formed to rob capacity from the cathode. The extrinsic electronic conductivity of the electrode material was enhanced by carbon coating; the intrinsic conductivity is improved by doping Nb for Ti as is demonstrated for $Ti_{0.9}Nb_{0.1}Nb_2O_7$.

■ ASSOCIATED CONTENT

Supporting Information. Experimental details and supplementary figures (PDF). This material is available free of charge via the Internet at http://pubs.acs.org.

■ AUTHOR INFORMATION

Corresponding Author

*Tel: (512) 471-1646. E-mail: jgoodenough@mail.utexas.edu.

Present Addresses

[§]Lujan Center, LANSCE, Los Alamos National Laboratory.

■ ACKNOWLEDGMENT

This work was supported by Office of Vehicle Technologies of the U.S. Department of Energy under Contract No. DE-AC02-05CH11231 and the BATT Program Subcontract No. 6805919.

■ REFERENCES

(1) Peled, E.; Tow, D. B.; Merson, A.; Gladkich, A.; Burstein, L.; Golodnitsky, D. *J. Power Sources* **2001**, *97*−*8*, 52–57.

(2) Hu, J.; Li, H.; Huang, X. *Solid State Ionics* **2007**, *178*, 265–271.

(3) Li, L. F.; Xie, B.; Lee, H. S.; Li, H.; Yang, X. Q.; MeBreen, J.; Huang, X. J. *J. Power Sources* **2009**, *189*, 539–542.

(4) Kang, S. H.; Abraham, D. P.; Yoon, W. S.; Nam, K. W.; Yang, X. Q. *Electrochim. Acta* **2008**, *54*, 684–689.

(5) Han, J. T.; Liu, D. Q.; Song, S. H.; Kim, Y.; Goodenough, J. B. *Chem. Mater.* **2009**, *21*, 4753–4755.

(6) Wadsley, A. D. *Acta Crystallogr.* **1961**, *14*, 660.

(7) Gasperin, M. *J. Solid State Chem.* **1984**, *53*, 144–147.

(8) Kavan, L.; Grätzel, M. *Electrochem. Solid-State Lett.* **2002**, *5*, A39–A42.